EPR Studies of the Microscopic Structure of the (100) Si/SiO_2 Interface: Current Status and Perspectives

H.J. von Bardeleben and J.L. Cantin
Groupe de Physique des Solides
Universités Paris 6&7, CNRS
2, place Jussieu, 75005 Paris

Received February 22, 1997

I. Introduction

Due to their technological importance in microelectronic devices the microscopic structure of the Si/SiO_2 interface has been intensively studied for over 30 years by numerous experimental techniques[1,2]. Generally these studies focussed on the analysis of the crystallographic structure of the first monolayers of SiO_2 at the interface and its lateral in-plane as well its vertical evolution. Depending on the experimental technique employed the vertical resolution, which can be obtained, varies widely and the precise meaning of the term "interface" depends on the technique used. Examples are given by the TEM[3], XPS[4-6] and EPR[7-9] techniques, which probe the interface with monolayer resolution and optical[10] and ion beam techniques[11,12], which probe an average interface region of several monolayers thickness.

Most of the experimental techniques analyze the defect free part of the interface, but in particular the electron paramagnetic resonance and electrical measurements have also allowed to assess quantitatively the interface point defects[13], which are attributed to Si dangling bond defects. As we will show later, these defects can be useful for interface studies as- they are local probes for the surrounding SiO_2 structure. Given the different crystal structures of Si and SiO_2 and its very different interatomic distances one might naively expect that the formation of the interface will only be possible with the development of high defect densities. Surprisingly however, inspite of the difference in the Si and SiO_2 crystal structures only $\approx$1% of the Si interface atoms are not bonded and introduce electrically active defects.

In the following we will limit our discussion to the case of the (100) Si/SiO_2 interface obtained by high temperature thermal oxidation, which is at the base of most applications, but which due to experimental difficulties has been much less studied by the EPR technique in the past than the (111) Si/SiO_2 interface.

II. Structural information by electron microscopy and XPS

Contrary to the case of isostructural interfaces such as Si/SiGe for example, the complexity of the Si/SiO_2 interface is not only related to the difference in the lattice structures of crystalline SiO_2 (quartz, tridymite or betacristobalite) and Si, but in addition to the fact that the interface is the interaction layer in the thermal oxidation processs; it is thus continously modified during the growth of the SiO_2 layer, which with the exception of the first monolayers at the interface is amorphous. Two types of structural informations are generally obtained: the first one concerns the microstructure of the defect free part of the interface and the second of these

regions, where the transition is accompanied by point defect formation.

When modelling the Si/SiO_2 interface both abrupt interfaces and extended interface regions with a thickness of ≈10Å have been considered. In the second case the interface is a transition region containing silicon atoms in intermediate oxidation states Si^{1+} (O-Si–Si_3), Si^{2+} (O_2=Si=Si_2) et Si^{3+} (O_3 ≡Si-Si) and being of oxygen deficient stoichiometry SiO_{2-x}. In the following we will give a rapid overview of the experimental results obtained and the interface models derived from these studies. Among the experimental techniques used High Resolution Transmission Electron Microscopy (HR TEM) and Photoemission Spectroscopy (PES) have been most widely applied.

We will first focus on studies, which have lead to the model of abrupt interfaces. As the density of atoms in the silicon (100) plane is approximately two times higher than in the (001) plane of α-quartz, a naive rigid fit of the SiO_2 structure to the Si(001) surface is expected to generate 50% of dangling bonds in the interface plane; in order to reduce the defect density the bond angles in SiO_2 network have to be modified. TEM is off course well suited and has been used to determine the arrangement of the first monolayers at the interface and to detect irregularities. Whereas all observations of thermally grown interfaces report rather flat interfaces, the vertical extension of the interface, related to the silicon suboxides present, is difficult to determine. One of the first results was obtained by A. Ourmazd et al.[3,14] who performed HR TEM and Transmission Electron Diffraction on interfaces thermally grown on atomically flat (001) Molecular Beam Epitaxy (MBE) grown silicon substrates. They simulated the contrast of the HR TEM images and the diffraction patterns and proposed the existence of a cristalline (tridymite) SiO_2 interface layer (Fig.1a). The tridymite layer is oriented with respect to the Si substrate such that its [010] axis is parallel to the [001] direction of the Si and its [100] axis is parallel to the Si [110] direction; in this case we have a mismatch of 13.2%; in the [002] direction parallel to the Si [110] axis this leads to a mismatch of 6.7%. The epitaxial growth of tridymite is also possible in a slightly different configuration, shifted by 0.5 a.u. along the Si[110] direction; both configurations were observed simultaneously at the interface. This cristalline SiO_2 phase is found to be limited to a only ≈5Å thick interface region. The abrupt transition between the silicon and the tridymite leaves silicon unsaturated bonds at the interface. These bonds have to be supposed to be dimerized in order to reduce the otherwise large total density of dangling bonds, which would contradict the relatively low density of interface state measured electrically (≈1%).

The interface studies in low temperature grown thermal and native oxides by X-Ray grazing incidence diffraction[15] and HR TEM techniques also suggested the existence of crystalline forms of SiO_2. The cristalline structure proposed is cubic and similar to the bulk cristobalite phase. T.A. Rabedeau et al.[16] also performed X-Ray grazing experiments on interfaces grown on Si substrates deposited by MBE. Scattering data evidenced a 2×1 epitaxial structure at the interface, but concerning only approximately 10% of the total interface. As this interface reconstruction is improbable, if the cristalline SiO_2 is tridymite or cristobalite phase, T.A. Rabedeau and al. proposed an abrupt interfacial structure, locally reconstructed by dimerization of Si bonds as shown in Fig. 1b. This interface reconstruction is analogous to the one occuring at the (001) Si surface. More recently the model of a pseudo cristobalite phase has found more support by X-ray diffraction measurements[17]; these authors observed additional diffraction peaks, which they modelled with a tetragonally distorted β cristobalite phase.

Extended interfaces have been proposed following the observation of silicon sub oxides, which are detected by techniques sensitive to the chemical bonding of silicon. The field ion microprobe[18] is such a technique able to measure the local O/Si ratio. The observed ratio differs from 2 over a width of 3 to 5Å, i.e. two atomic layers. By PES, F.J. Himpsel and et. al.[5] measured three different suboxides of silicon at the interface via the chemical shift of the Si 2p core level. For thermal oxides interfaces, the measured density of Si atoms in intermediate oxidation states is high, of the order of

$10^{15}/cm^2$. Based on these results the authors proposed an interface model, in which the transition between Si and SiO_2 is supposed to occur over two monolayers of SiO_x as shown in Fig. 1c. The amount of suboxides is related to the roughness of the interface. Contrary to abrupt interface models, this model does not lead to unsaturated Si bonds.

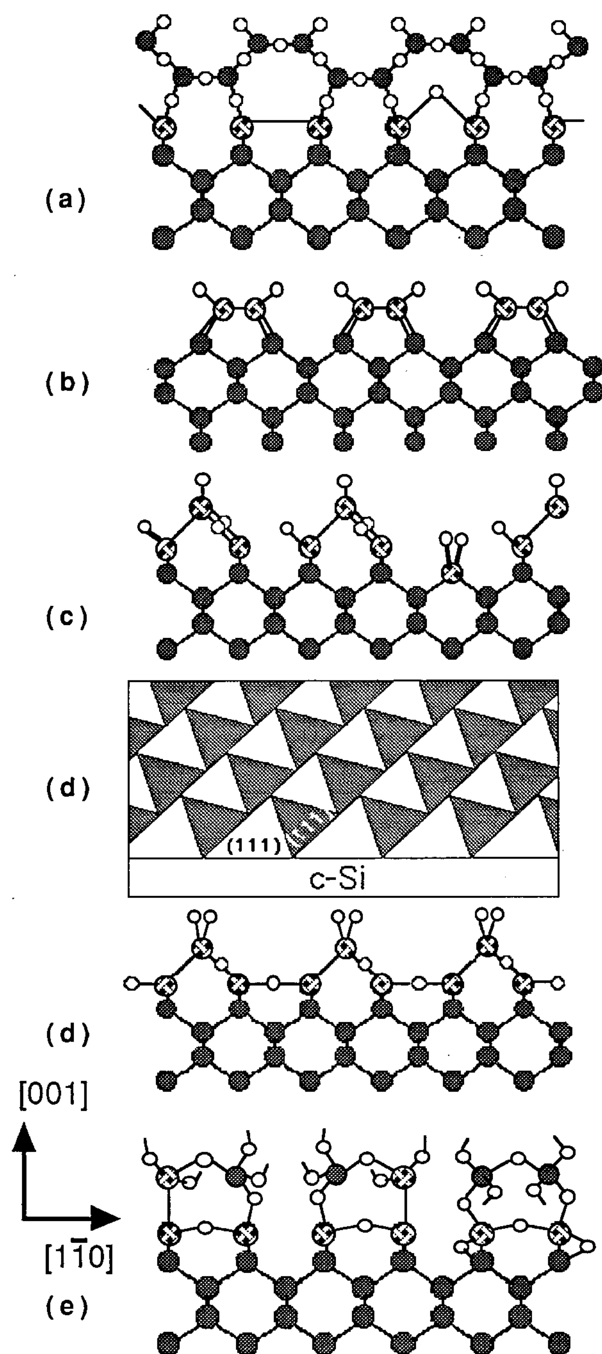

Figure 1. Interface models proposed by (a) Ourmazd[14], (b) Rabedeau[16], (c) Himpsel[5], (d) Ohdomari[19], (e) Pasquarello[20].

III. Models

I. Ohdomari and al.[19] proposed a different model for the (001)Si/SiO_2 interface tailored to minimize the distortion energy of the different networks. Their calculations showed that the occurence of (111)Si facets at the (100) interface should be energetically favourable. They thus proposed a model in which the entire interface was facetted with pyramids of (111) faces and 4 atomic layers height (Fig. 1d). This model is not able to take into consideration the silicon suboxides distribution deduced from the XPS studies. Subsequently these authors proposed several modified models, in which the (111) faceted (001) interface is mixed with regions containing silicon sub oxides.

Recently, A. Pasquarello and al[20,21] reconsidered the abrupt interface obtained by connecting a (distorted) tridymite phase to the bulk Si (001) surface. This is the model already proposed by Ourmazd et al[3,14] on the basis of their high resolution TEM results (Ourmazd model, Fig. 1a). Pasquarello et al tried to reconcile their structure with the two main experimental informations: the suboxide distribution as deduced from XPS and the low dangling bond density known from EPR and electrical studies. In order to achieve this, a transition region characterized by a bond angle and bond length distribution had to be introduced. Further, they had to allow for two defect configurations: oxygen bridging centers and Si-Si dimer configurations (Fig. 1e). The strain, estimated from the tetrahedral volumes of the different sub oxides is found to decrease rapidly away from the interface. The thickness of the transition region is estimated to 5Å.

It seems clear, that all rigid epitaxial models mentioned above always produce a large amount of Si dangling bonds at the interface, rarely less than one half of the interfacial Si atoms. This is in clear contradiction to the known interface state density of the Si/SiO_2 interface, for which the density of dangling bond is always $\leq$ 1% of the interface atoms. The abrupt interface models also fail to predict the existence of Si^{3+} sub oxide which

strongly suggests the presence of silicon protrusion in the silica, near the interface. On the other hand, the extended models are less defined and the knowledge of the distribution of sub oxide do not lead to an unique interfacial model.

IV. Interface defects: the P_{b0} and P_{b1} centers

(100)Si/SiO_2 interfaces can be formed by a variety of different procedures such as high temperature furnace oxidation of bulk silicon, rapid thermal oxidation, oxide deposition at intermediate temperatures in CVD systems or simply at room temperature by exposition to ambient conditions (native oxide). Off course, the interface structure will in addition depend on the surface preparation before the oxidation and might further vary with the oxide thickness. This is a a priori very complex situation; in spite of this, very similar experimental results as concerns the nature and concentration of the interface defects were obtained in all types of oxides. The (100) Si/SiO_2 interface, which has been studied in most detail, is the one formed by high temperature thermal oxidation; therefore in the following most of the discussion will be limited to this case.

The first EPR studies of the (100)Si/SiO_2 interface were reported by E.Poindexter et al in 1981[22]. They concerned thermal oxides formed by 800°C to 1000°C furnace oxidation of bulk silicon samples. The principal experimental result, which was extended and basically confirmed by the subsequent studies[7,8,9] is the simultaneous presence of two different interface defects, labeled P_{b0} and P_{b1}. In the case of (111) and (110) interfaces only one paramagnetic interface defect, the so called P_b center, had beeen detected. The P_{b0} defect has very similar spin Hamiltonian parameters as the P_b defect at the (111) Si/SiO_2 interface; the P_{b1} center on the contrary is characteristic for the (100) interface in the sense that it has not been observed for any other interface orientation. As the P_{b0} and P_{b1} centers have the symmetry of the silicon lattice they must be situated at the Si substrate side of the interface layer. These defects do not exist as volume defects in bulk Si. Poindexter et al proposed two simple microscopic models for these defects •Si-Si_3 and •$SiSi_2O$ Si dangling bond defects (Fig. 2).

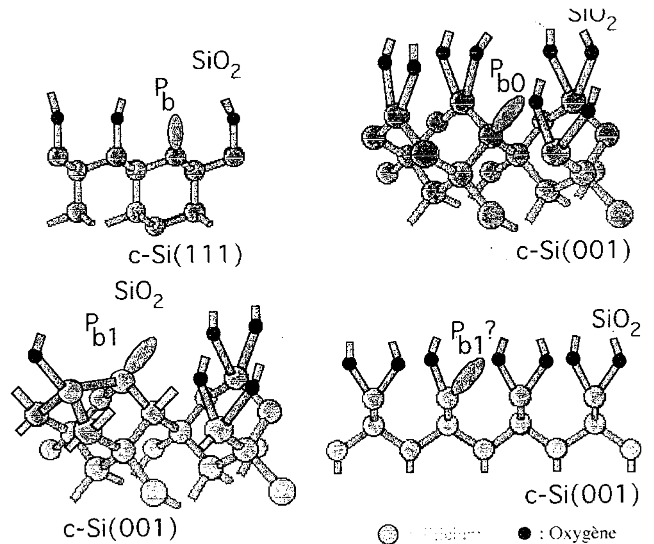

Figure 2: Interface defect models for the P_{b0} and P_{b1} defects by Poindexter[22], and Edwards[32].

Whereas the EPR technique is well suited for a quantitative study of point defects its application to interfaces was rendered difficult by the weak signal to noise ratio obtainable; the limitations arise from the maximum interface area of a typical EPR sample ($\approx$ 30mm^2) and the low interface defect concentration of $\approx 10^{12}$cm^{-2}; this concentration turned out to be rather insensitive to the oxidation conditions. As a further complication, the two EPR spectra of P_{b0} and P_{b1} overlap strongly and split in multiplets for all magnetic field orientation besides BII[100]. These experimental difficulties prevented a precise determination of the P_{b0} and P_{b1} EPR parameters, which are neccessary for modellisation of their microscopic structure. Due to the much improved experimental conditions obtainable with the use of oxidized porous silicon substrates a complete determination of the EPR prameters in particular of the P_{b1} defect has been achieved recently.

The P_{b0} defect is characterized by the following EPR parameters, which vary only slightly with the oxidation conditions:

Table 1

	P_{b0} center	Pb center[23]
Interface Orientation	(100) Si/SiO_2	(111) Si/SiO_2
spin	1/2	1/2
g-tensor: principal values	g1=2.0015 g2=g3=2.0087	gl=2.0013...2.0017 g2=g3=2.0087
orientation of principal axes	II[111], ⊥[111]	[111], ⊥[111]
p.t.p. linewidths (G) at X-band	1.5 for II[111] 3.0... 3.4 for ⊥[111]	1.2... 1.7 for II[111] 3.0...3.4 for ⊥[111]
point symmetry	C_{3v}	C_{3v}
number of differently oriented defects observed for B in (110)	3 or 4	1
Central ^{29}Si hyperfine $A_{\parallel}$ interaction ($10^{-4}cm^{-1}$) $A_{\perp}$	136...143 $10^{-4}cm^{-1}$ 73...79 10^{-4} cm^{-1}	146 x 10^{-4} cm^{-1} 85 x $10^{-4}cm^{-1}$

Surprisingly the EPR parameters for the P_{b0} defect at the (100) interface and the P_b defect at the (111) interface are identical. The small variations in g-values and linewidths are related to the type of oxide and the defect concentration, which can modify the linewidth and shape by dipolar interactions; they are not related to the interface orientation. The numerical values of the g-tensor and hyperfine interaction can be understood in a simple tight binding model[24] of a singly occupied sp^3 dangling bond orbital.

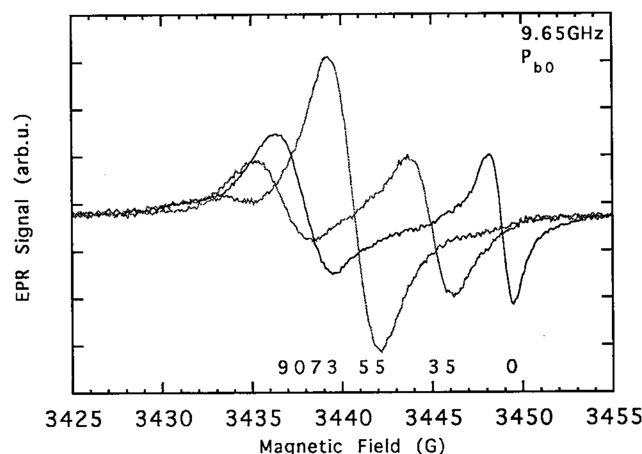

Figure 3: X-band EPR lines of the P_{b0} defect for various orientations of the magnetic field relative to the [111] axis; orientation dependant linewidth.

A particular property of the interface defects and thus also of the P_{b0} defect is an EPR linewidth, which varies with the orientation of the magnetic field (Fig.3). The peak-to-peak width of the first derivative spectrum takes at X-band values between 1.3G for BII[111] and 3.2G for B⊥[111]. From EPR studies at different microwave frequencies[25,26] (X-band, K- band, Q-band) it is known that the line broadening is in addition microwave frequency dependant; it must thus be attributed to a non resolved g-factor distribution, the origin of which is a variation of the local microscopic structure. These results are in good agreement with electrical measurements on interface defects, which have shown a broad distribution of energy levels in the gap[27,28].

The identification of the microscopic structure of the P_{b0} defect is mainly based on the observation of its central hyperfine interaction. All EPR measurements were performed on non isotopically enriched Si, which means samples with only 4.7% ^{29}Si atoms with a nuclear spin I=1/2. They give rise to a hyperfine doublet with ≈100 smaller intensity than the central line; such low intensity signal is unobservable under normal experimental conditions, i.e. when working with a single sample of ≈30mm^2 dimension. The first reported measurement on bulk (100) Si[8] required the use of a stack of 75 samples. And even in this case only one value of the A tensor- for the most favourable magnetic field orientation BII[001]- has been determined; from the intensity ratio of the hyperfine lines to the central lines it could be concluded that the wavefunction of the P_{b0} center is localized on one Si atom, in agreement with the Si dangling bond model. Later measurements on porous silicon have (Fig.4) allowed to extend these results and to determine the central hyperfine interaction

tensor[9,29,30]. They confirm the interaction of the electron with one ^{29}Si nucleus and the trigonal symmetry of the hyperfine tensor. The picture for P_{b0} of an isolated Si dangling bond defect is thus well confirmed.

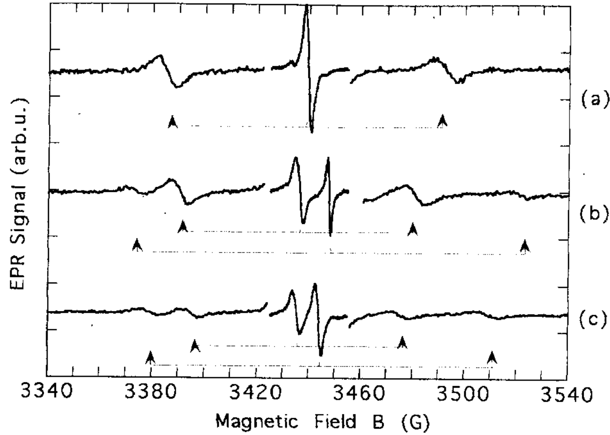

Figure 4: EPR spectrum of the ^{29}Si central hyperfine lines in oxidized porous Si for three magnetic field orientations (a) BII[001], (b) BII[111], (c) BII[110]; T=300K.

As concerns the P_{b1} defect its exact g tensor has only been determined recently[9,30]. The P_{b1} defect has a lower point symmetry than P_{b0}, i.e. monoclinic I. The lower symmetry leads to a higher orientation degeneracy of the EPR spectrum (Fig. 5); for a variation of the magnetic field in the (110) plane the P_{b1} EPR spectrum is composed of one or two lines for an atomically flat (100) interface and seven lines in the most general case (such as found in oxidized porous silicon), if all six interface planes ((100) or equivalent) are present (Fig.6). For each atomically flat interface (100) plane we have two distinguishably oriented P_{b1} defects. The use of oxidized porous silicon structures has greatly facilitated the EPR analysis of the P_{b1} EPR spectrum. The EPR parameters are resumed in Table 2. In spite of an in principle sufficient signal to noise ratio it has not been possible to detect the central hyperfine lines; we ascribe this to a reduced value of the hyperfine constant - as compared to P_{b0} - so that the hyperfine lines are hidden in the wings of the central lines; these results do not confirm the only previous measurement reported by Brower[8].

Table 2

P_{b1} Center				
spin S	1/2			
principal values of g-tensor	g1	g2	g3	effective g value for BII[100]
Ref.[9,30]	2.0058	2.0029	2.0069	2.0041 2.0058
Ref. [31]	2.0058	2.0020	2.0084	2.0041
Ref. [22]	2.0052	2.0012	2.0081	2.0035
principal axes of g-tensor	g1	g2	g3	
Ref. [9,30]	[011]	[211]	[111]	
ptp linewidth (G)	3.8....4.2 G [9,30]			
concentration	$\approx 1 \times 10^{12}$cm^{-2}			

Whereas it is common practice, to speak of the P_{b0} or the P_{b1} defect we should be aware that we have to do actually with a distribution of defects, which at X-band EPR spectroscopy can not be distingushed. Contrary to the case of volume defects in cristalline Si or SiO_2 for example both interface defects are characterized by a distribution of the spin Hamiltonian parameters (g-tensors, hyperfine tensors), which reflect continously varying locally different microscopic configurations. The evidence comes from the orientation and frequency dependent EPR linewidths (Fig. 7), which give a measure of the g-factor distribution. As this distribution is small as compared to the g-value differences, the only manifestation are linebroadening effects;

therefore these defects lead nevertheless to distinct rotation patterns for their respective EPR spectra, which allow quantitative evaluations. In the case of P_{b1} the orientation dependence of the EPR line widths is not pronounced at X-band frequencies. Basically isotropic linewidths of (4.0 ± 0.3)G are observed in porous oxidized silicon. However, a change of the microwave frequency from 9GHz to 35GHz shows once again an increase of the linewidths by ≈ 4, confirming the distribution of local environments also for the P_{b1} defect[26].

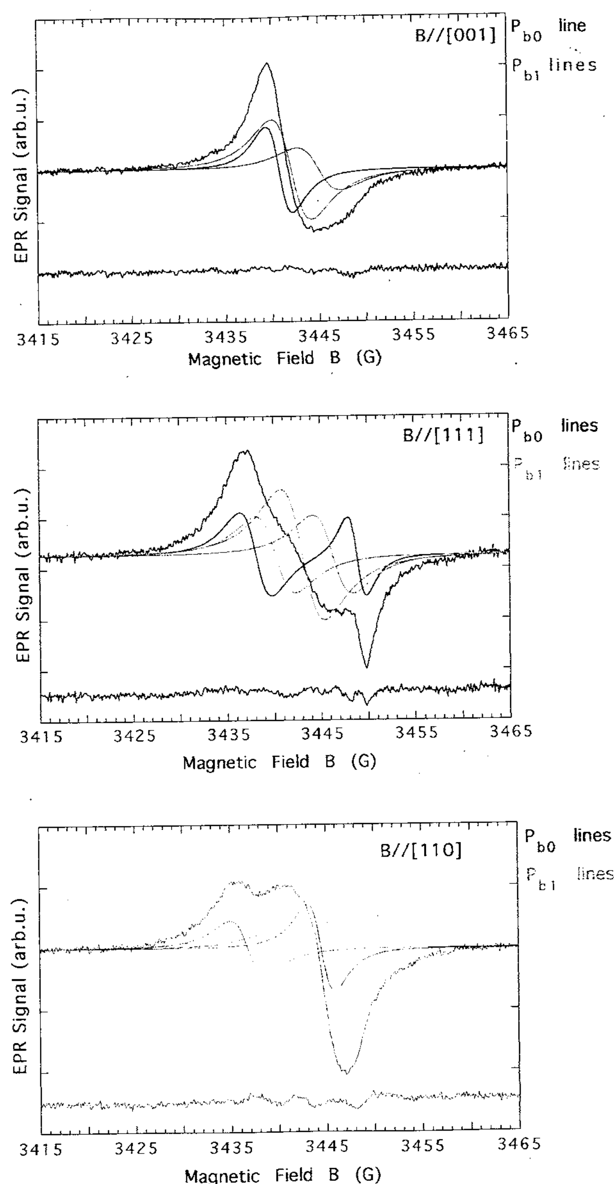

Figure 5: Experimental EPR spectra of the mixed $P_{b0}P_{b1}$ spectra and their decomposition in P_{b0} and P_{b1} lines in oxidized porous Si for three magnetic field orientations (a) BII[001], (b) BII[111], (c) BII[110]; T=300K.

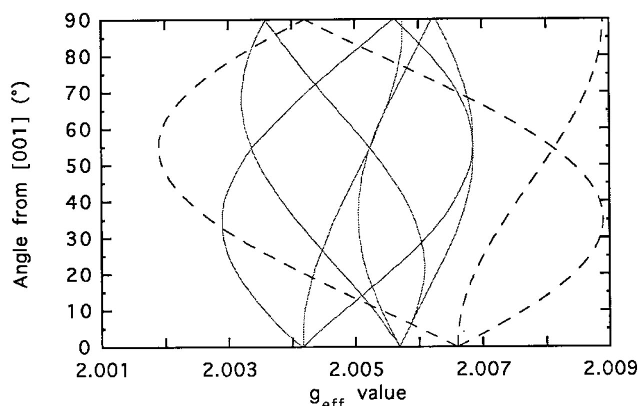

Figure 6: Angular variation of the effective g-value of the P_{b0} (dashed) and P_{b1} (solid) EPR spectra for a rotation of B in the (110) plane.

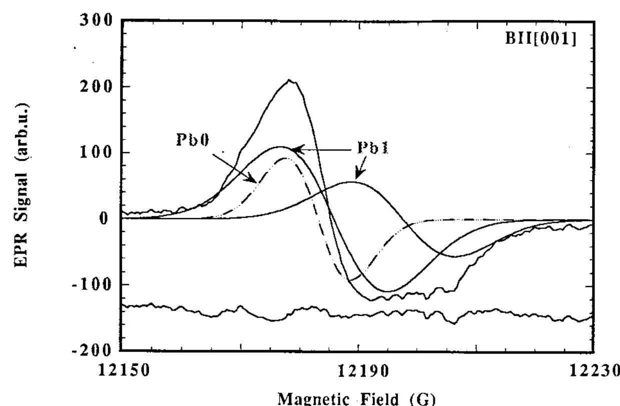

Figure 7: Experimental Q-band EPR spectrum in oxidized porous Si and its decomposition in P_{b0} and P_{b1} lines for BII[001]; the lines are broadened by ≈ 4 as compared to X-band spectra.

Microscopic Models

Among the main elements allowing the establishment of microscopic models are the central and ligand hyperfine interaction as well as the point symmetry of the defects. The symmetry properties of the P_{b0} and P_{b1} defects allow their attribution to a Si lattice related point defect located at the interface. Whereas for the P_{b0} center the hyperfine interactions with the central atom and the Si neighbours have been determined, for the P_{b1} defect such measurements are not available. The only information we dispose of is a lower value of the central hyperfine interaction[8], as compared to the one of P_{b0}.

The P_b center at the (111)Si/SiO_2 interface has been convincingly attributed to a Si dangling bond defect of a threefold coordinated •Si-Si_3 center; the similitude of the spin Hamiltonian parameters of the P_{b0} center

can and have been taken as a proof for an identical microscopic structure (Fig.2). At an atomically flat (100) interface the presence of threefold coordinated P_{b0} defects would a priori not be expected. To allow for such defects different models have been considered: if the (100) interface is facetted with (111) planes, as has been proposed by Odhomari[19] on the basis of different experimental observations, the observation of interface defects characteristic for (111) interfaces is no longer surprising. Unfortunately systematic EPR studies on interfaces purposely prepared to favour or minimize facetting have not been reported. A priori more complicated models cannot be excluded: for example one might also assume an extended interface region containig threefold coordinated Si-Si_3 complexes. To agree with the experimental results one must however assume that the symmetry axis of such complexes should stay aligned within $\leq 5°$ with the [111] directions of the Si substrate. In fact, this seems not very probable and such a model has not found serious consideration.

We can further analyze the information contained in the mutliplicity of the EPR spectrum: in the simple case of an atomically flat (111) interface for example we should observe only one P_b center orientation, the one for which the dangling bond orbital is oriented normal to the interface plane. If we allow for facets at the (100) interface up to four differently oriented facets (111), (-1 -1 1), (1 -1 -1), (-1 1 -1) can be expected. For an arbitrary orientation of the magnetic field relative to the crystal axes the EPR lines of each facet arises at different positions and can thus be separatly evaluated. Such detailed analyses of the EPR spectra are generally not reported and only the spectrum for the high symmetry orientation of the magnetic field BII[001], for which the resonances of all four potentially differently oriented P_{b0} centers occur at the same magnetic field position, is given. Nevertheless already the first observations by Poindexter et al[22] showed the presence of all four P_{b0} orientations at the (100) interface.

As concerning the microscopic model for the P_{b1} center, the original proposition of Poindexter, a (Si-Si_2O) Si dangling bond defect, has found not to be in agreement with the electrical properties of the P_{b1} defect. The available results favour instead the Si-Si dimer model of Edwards[32], which apparently fits all exprimental results and must be considered at this moment as the best model for the P_{b1} center.

Defect concentrations

The concentrations of both interface defects P_{b0} and P_{b1} in hydrogen free samples are in the range of 1...3 $10^{12}cm^{-2}$ [22,25,33]. It can be expected, that as in the case of (111) interfaces, this concentration depends on the oxidation conditions and post annealing treatments, but no systematic studies have been reported. Apparently it is not possible to prepare (100) interfaces with exclusively P_{b0} or only P_{b1} defects. The relative intensities of the P_{b0} and P_{b1} defects turned often out to be of the order of 1. Nevertheless this ratio does not seem to be related to a particular surface preparation or specific oxidation conditions. Whereas for the (111) interface a "universal" defect concentration related to the oxidation temperature and post growth annealings has been proposed[34], no such information is known for the (100) interface. However, all studies seem to indicate an about three times lower total defect density than at (111) interfaces. The in device structures often reported apparently much lower defect concentrations of $\approx 10^{10}cm^{-2}$ are of course only due to the passivation of the interface defects by hydrogen; their total concentration rests unchanged.

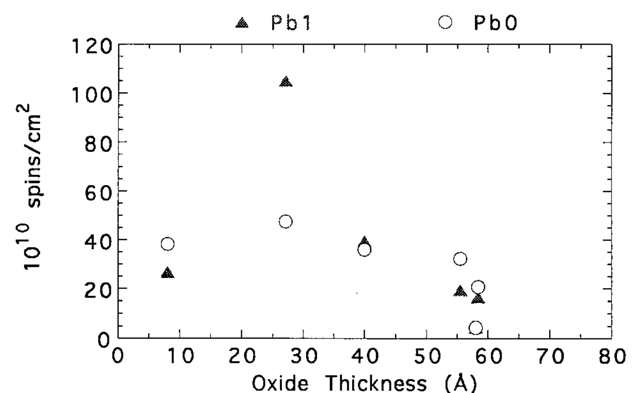

Figure 8: Interface defect concentration (P_{b0}, P_{b1}) as a function of oxide thickness for 1000°C furnace oxidized porous Si.

Some insight in the formation mecanism of P_{b1} centers was obtained by the evaluation of the P_{b0}, P_{b1} concentrations in ultrathin oxides of varying thickness[9]. The results (Fig.8) show, that the P_{b1}/P_{b0} ratio can be different from 1 but only in the very inital state of oxide fornation; for oxide thicknesses inferior to

20Å P_{b1}/P_{b0} intensity ratios of up to 6 have been observed. For higher oxide thicknesses the P_{b1} concentration diminishes and approaches the thick oxide case of $P_{b1}/P_{b0} \approx 1$. Within the Edwards model[31] for P_{b1} (Si-Si dimer dangling bond defect), this transformation can be understood as a reduction of the number of Si-Si dimer configurations and their replacement by Si-O bridges in the course of the interface formation.

Electrical Properties of the Pb interface defects

Since the earliest measurements of the Pb centers their relation with the electrically active defects characterized by C(V), DLTS and charge pumping techniques has been considered[22,27,28,35].In the first studies the total defect concentrations of electrically active interface defects and Pb centers were quantiatively compared. Later, more sophisticated schemes were applied in order to determine in addition the energy level position of the Pb centers.

Whereas there is no doubt, that the total concentration of Pb centers, which is in the 1×10^{12}cm^{-2} range, is close to the electrically determined interface state density, the question of whether there is a 1:1 relationship or whether we have in addition electrically active non paramagnetic defects is still under discussion. It might well be, that the answer to this question really depends on the particular oxide grown and that a global answer is not appropriate. Already the first results reported by Poindexter et al[22] had shown two different cases for "fast pulled" and "cooled" oxides with respectively ratios of 1:1 and 2:1.

Gerardi et al[25] measured the P_{b0}, P_{b1} center concentrations as a function of the Fermilevel position by applying a polarisation during the EPR measurement: Combining the results of electrical measurements and bias dependent EPR they attributed two energy level distributions (Fig.9) to each of the two defects, which are thus two electron centers. The levels have peak postions at $E_v + 0.30$ eV and $E_v + 0.85$eV (P_{b0}) and $E_v + 0.45$eV and $E_v + 0.80$eV (P_{b1}) respectively. The distributions are large (Gaussian distribution with a standard deviation of 0.1eV) and with different widths for the two charge states.

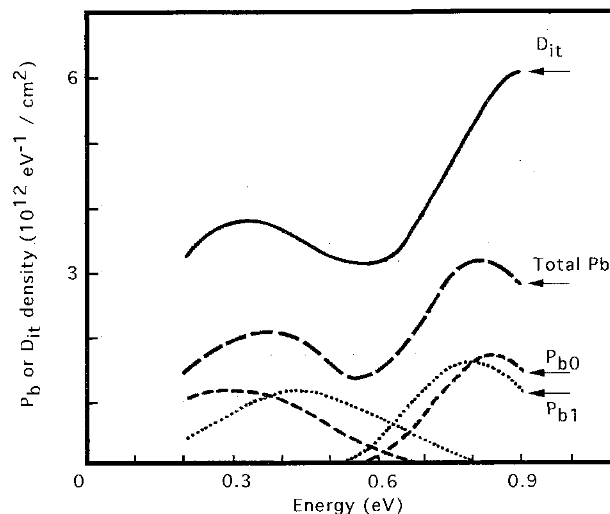

Figure 9: Comparison of total interface defect density and the P_{b0} and P_{b1} center densities as a function of energy.

V. Defect Passivation by Hydrogen

Only few EPR studies of the Pb center passivation by hydrogen have been reported for (100) interfaces[33,36–38]. The results are not easy to compare due to the extremely different cases studied: the first case[37] concerns a 675Å thick oxide grown at 900°C and passivated by exposure at room temperature to atomic hydrogen; in the second case an ultrathin (20Å) oxide was grown at a low temperature of 176°C and exposed to molecular hydrogen. The results of the first study are unexpected: exposure to hydrogen free previously vacuum annealed samples with defect concentrations of 5×10^{11}cm^{-2} (P_{b0}) and 4.2×10^{11}cm^{-2} (P_{b1}) does not lead to any significant passivation of neither the P_{b0} nor the P_{b1} center. However, if previously passivated samples are exposed to atomic hydrogen a depassivation of both P_b centers is observed. In the second study[38] - applying exposure to molecular hydrogen at temperatures of 200°C - very similar passivation kinetics have beeen observed for the two Pb centers. The initial Pb center concentration were 8.4 10^{12}cm^{-2} and 4×10^{12}cm^{-2} for P_{b0} and P_{b1} respectively. Passivation was performed in the 220°C temperature range under 1.1atm H_2. The process has been attributed to a simple P_b-H_2 reaction and the relevant passivation parameters have been determined. They are characterized by thermal activation energies of 1.51 and 1.57

eV respectively, assuming an identical pre-exponential factor of 1.43×10^{-6} cm^3s^{-1} for both centers. The two other more qualitative studies concerned passivation by forming gas and moist air and allow no insight in the passivation process.

VI. Degradation of interfaces and Pb centers

The degradation of interfaces by ionizing irradiation and high field stressing has been studied in detail by electrical techniques. The main result concerning the interface states is that both processes lead to a depassivation of the initially hydrogen passivated Pb centers; in fact many details of the quantitative relationship between the degradation and Pb center passivation have been studied: they concern parameters such as type of degradation, temperature, polarisation of the MOS structures, oxide quality and thickness, initial state of the interface defects. The basic idea contained in most models is an interaction of atomic hydrogen with passivated Pb centers leading to molecular hydrogen formation and electrical activation of Pb centers. The published EPR and spin dependent recombination (SDR) studies[39−41] suffer however from unsufficiently analyzed Pb center spectra, which donot allow to give quantitative results separately for P_{b0} and P_{b1}. Once again evidence that the Pb centers are not the only electrically active interface defects[28]. We have recently studied the effect of X-ray and γ irradiation on Pb centers in ultrathin oxides using oxidized porous Si. Our results for non hydrogen passivated samples indicate both defect formation and passivation effects; in the first stage of irradiation we observe as expected degradation, i.e. an initial increase of the paramagnetic Pb center concentration; however for high doses of irradiation a strong decrease of the paramagnetic interface defect concentration is observed (Fig.10). Studies with similar results have been performed by K. Awazu et al[42]. More systematic EPR studies with a selective analysis of the role of P_{b0} and P_{b1} defects in degradation mecanism are clearly required.

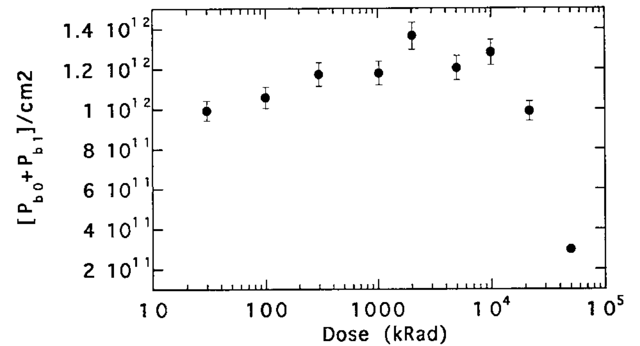

Figure 10: Variation of the total interface defect (Pb) density as a function of γ irradiation dose (SiO_2) in oxydized porous Si as measured by EPR.

VII. Perspectives

Whereas many experimental details on the (100) Si/SiO_2 interface defects have been accumulated in more than 15 years of studies, many challenges still exist. To cite the most important, the microscopic structure of the P_{b1} defect, which needs further confirmation and the defects and cristalline structure or disorder of the first monolayers of SiO_2 at the interface. The potential strength of oxidized porous silicon might be the tool for further more sophisticated studies such as electron nuclear double resonance in ^{17}O enriched samples to resolve these problems. A new field emerging is the one of ultrathin SiO_2 layers, which give additional experimental challenges. More complicated interface structures as obtained after mixed oxide/nitride formation must be studied by EPR in the future. The EPR technique should also be well adapted to tackle the role of deuterium in the degradation of D passivated MOS structures.

References

for reviews see for example:

1. Semicond. Science & Technology 4, (1989).
2. *The Physics and Chemistry of SiO_2 and the Si-SiO_2 Interface-3*, H.Z. Massoud, E.H. Poindexter, C.R. Helms, Eds. (The Electrochemical Society, Inc., Los Angeles, 1996).
3. A. Ourmazd, J.A. Rentschler, J. Bevk Appl. Phys. Lett. **53**, 743 (1988).
4. P.J. Grunthaner, M.H. Hecht, F.J. Grunthaner, N.M. Johnson J. Appl. Phys. **61**, 629 (1987).
5. F.J. Himpsel, F.R. McFeely, A.Taleb-Ibrahimi, J.A. Yarmoff Phys. Rev. B**38**, 6084 (1988).

6. F. Rochet, M. Froment, C. D'Anterroches, H. Roulet, G. Dufour, Philos. Mag. B **59**, 339 (1989).
7. E.H. Poindexter and P.J. Caplan Prog. in Surface Science **14**, 201 (1983).
8. K.L. Brower, Zeitschrift fuer Physikalische Chemie NF 151,177(1987).
9. J.L. Cantin, M. Schoisswohl, H.J.von Bardeleben, V. Morrazzani, J.J. Ganem, I.Trimaille in *The Physics and Chemistry of* SiO_2 *and the Si-*SiO_2 *Interface-3* ed. by H.Z. Massoud, E.H. Poindexter, C.R. Helms (The Electrochemical Society, Inc., Los Angeles, 1996),p.28.
10. K.J. Hebert, T. Labayen, E.A. Irene in *The Physics and Chemistry of* SiO_2 *and the Si-*SiO_2 *Interface-3* ed. by H.Z. Massoud, E.H. Poindexter, C.R. Helms (The Electrochemical Society, Inc., Los Angeles, 1996),p.81.
11. J.J. Ganem, G. Battistig, S. Rigo, I.Trimaille Appl. Surf. Sci. **65/66**, 647 (1993).
12. E.P. Gusev, H.C. Lu, T. Gustafsson, E. Garfunkel Phys. Rev. B**52**, 1759 (1995).
13. G.J. Gerardi, E.H. Poindexter, P.J. Caplan, N.M. Johnson Appl. Phys. Lett. **49**, 348 (1986).
14. A. Ourmazd, D.W. Taylor, J.A. Rentschler, J. Bevk Phys. Rev. Lett. **59**, 213 (1987).
15. P.H. Fuoss, L.J. Norton, S. Brennan, A. Fischer-Colbrie Phys. Rev. Lett. **60**, 600 (1988).
16. T.A. Rabedeau, I.M. Tidswell, P.S. Pershan, J. Bevk, B.S. Freer Appl. Phys. Lett. **59**, 706 (1991).
17. T. Shimura, I. Takahashi, J. Harada, M. Umeno in *The Physics and Chemistry of* SiO_2 *and the Si-*SiO_2 *Interface-3* ed. by H.Z. Massoud, E.H. Poindexter, C.R. Helms (The Electrochemical Society, Inc., Los Angeles, 1996),p.456.
18. A. Cerezo, C.R.M. Grovenor, G.D.W. Smith J. Microsc. (Oxford) **141**, 155 (1986).
19. I. Ohdomari, H. Akatsu, Y. Yamakoshi, K. Kishimoto J. Appl. Phys. **62**, 3751 (1987).
20. A. Pasquarello, M.S. Hybertsen, R. Car, Phys. Phys. Lett. **74**, 1024 (1995).
21. A. Pasquarello, M.S. Hybertsen, R. Car, Appl. Phys. Lett. **68**, 625 (1996).
22. E.H. Poindexter, P.J. Caplan, B.E. Deal, R.R. Razouk, J. Appl. Phys. **52**, 879 (1981).
23. A. Stesmans Semicond. Science & Tennology **4**, 1000 (1989).
24. M. Lannoo, J.C. Bourgoin, Physica **116B**, 85 (1983).
25. K.L. Brower, Phys. Rev. B **33**, 4471 (1986).
26. J.L. Cantin, H.J.von Bardeleben unpublished.
27. G.J. Gerardi, E.H. Poindexter, P.J. Caplan, N.M. Johnson Appl. Phys. Lett. **49**, 348 (1986).
28. J.L. Autran, C. Chabrerie, P. Paillet, O. Flament, J.L. Leray, J.C. Boudenot, IEEE Trans. Nucl. Science **43**, 1996.
29. H.J.von Bardeleben, D. Stievenard, A. Grosman, C. Ortega, J. Siejka, Phys. Rev. B**47**, 10899 (1993).
30. J.L. Cantin, M. Schoisswohl, H.J.von Bardeleben, N. Zoubir, M. Vergnat, Phys. Rev. B**52**, 11599 (1995).
31. A. Stesmans, J. Braet, J. Wiotters, R.F. Dekeersmaecker, Surface Science **141**, 255 (1984).
32. A.H. Edwards, *The Physics and Chemistry of* SiO_2 *and the Si-*SiO_2 *Interface,* C.R. Helms, B. Deal Eds. (The Electrochemical Society, Atlanta, 1988),p.271.
33. J.H. Stathis, D.A. Buchanan, D.L. Quinlan, A.H. Parsons, D.E. Kotecki Appl. Phys. Lett. **62**, 2682 (1993).
34. A. Stesmans, G.van Gorp Phys. Rev. B**42**, 3765 (1990).
35. N.M. Johnson, D.K. Biegelson, M.D. Moyer, S.T. Chang, E.H. Poindexter, P.J. Caplan, Appl. Phys. Lett. **43**, 563 (1983).
36. J.H. Stathis, L. Dori, Appl. Phys. Lett. **58**, 1641 (1991).
37. J.H. Stathis, E. Cartier, Phys. Rev. Lett. **72**, 2745 (1994).
38. A. Stesmans, Solid State Commun. **97**, 255 (1996).
39. Y.Y. Kim, P.M. Lenahan, J. Appl. Phys. **64**, 3551 (1988).
40. J.T. Krick, P.M. Lenahan, G.J. Dunn Appl. Lett. **59**, 3437 (1991).
41. J.H. Stathis, D.J. DiMaria, Appl. Phys. Lett. **61** 2887 (1992).
42. K. Awazu, K. Watanabe, H. Kawazoe, J. Appl. Phys. **73**, 8519 (1993).